◆ Human Brain Mapping 37:1091–1102 (2016) ◆

Phasic and Sustained Brain Responses in the Amygdala and the Bed Nucleus of the Stria Terminalis during Threat Anticipation

Martin J. Herrmann,[1]* Stephanie Boehme,[1] Michael P.I. Becker,[2] Sara V. Tupak,[2] Anne Guhn,[1] Brigitte Schmidt,[1] Leonie Brinkmann,[2] and Thomas Straube[2]

[1]*Department of Psychiatry, Psychosomatics and Psychotherapy, University Hospital Würzburg, Fuechsleinstraße 15, Würzburg, D-97080, Germany*
[2]*Institute of Medical Psychology and Systems Neuroscience, University of Muenster, Von-Esmarch-Str. 52, Muenster, D-48149, Germany*

Abstract: Several lines of evidence suggest that the amygdala and the bed nucleus of the stria terminalis (BNST) are differentially involved in phasic and sustained fear. Even though, results from neuroimaging studies support this distinction, a specific effect of a temporal dissociation with phasic responses to onset versus sustained responses during prolonged states of threat anticipation has not been shown yet. To explore this issue, we investigated brain activation during anticipation of threat in 38 healthy participants by means of functional magnetic resonance imaging. Participants were presented different visual cues indicated the temporally unpredictable occurrence of a subsequent aversive or neutral stimulus. During the onset of aversive versus neutral anticipatory cues, results showed a differential phasic activation of amygdala, anterior cingulate cortex (ACC), and ventrolateral prefrontal cortex (PFC). In contrast, activation in the BNST and other brain regions, including insula, dorsolateral PFC, ACC, cuneus, posterior cingulate cortex, and periaqueductal grey was characterized by a sustained response during the threat versus neutral anticipation period. Analyses of functional connectivity showed phasic amygdala response as positively associated with activation, mainly in sensory cortex areas whereas sustained BNST activation was negatively associated with activation in visual cortex and positively correlated with activation in the insula and thalamus. These findings suggest that the amygdala is responsive to the onset of cues signaling the unpredictable occurrence of a potential threat while the BNST in concert with other areas is involved in sustained anxiety. Furthermore, the amygdala and BNST are characterized by distinctive connectivity patterns during threat anticipation. *Hum Brain Mapp 37:1091–1102, 2016.*

Key words: phasic and sustained fear; fMRI; amygdala; BNST; insula

Contract grant sponsor: German Research Foundation; Contract grant number: DFG: SFB-TRR-C06

Martin J. Herrmann and Stephanie Böhme contributed equally to this work.

*Correspondence to: Martin J. Herrmann, Laboratory of psychophysiology and functional imaging, University Hospital Würzburg; Fuechsleinstraße 15; D-97080 Würzburg, Germany. E-mail: herrmann_m@ukw.de

Received for publication 29 July 2015; Revised 12 November 2015; Accepted 3 December 2015.

DOI: 10.1002/hbm.23088
Published online 17 December 2015 in Wiley Online Library (wileyonlinelibrary.com).

INTRODUCTION

Animal research suggests a differential role of the amygdala and the bed nucleus of the stria terminalis (BNST), a part of the so-called extended amygdala, in anxiety [e.g. Davis et al., 2009; Walker et al., 2003]. While the amygdala seems to be involved in rapid fear responses to imminent threat and especially to fear-conditioned stimuli, the BNST is thought to modulate rather sustained anxiety states during unpredictable situations [e.g. Kalin et al., 2005; Walker et al., 2003]. Indeed, animal as well as human studies indicate that the BNST is more involved in sustained fear or anxiety. The inhibition or lesion of the BNST leads to reduced anxiety in anxiety provoking paradigms [e.g. Duvarci et al., 2009; Fendt et al., 2003; Hammack et al., 2004; Waddell et al., 2006]. In contrast, experimental stimulation of the BNST indicates physiological and behavioral manifestations of anxiety [Casada and Dafny, 1991; Dunn, 1987; Lungwitz et al., 2012; Sink et al., 2011, 2013; Walker et al., 2003] and BNST activation seems to be associated with increased anxiety [Kalin et al., 2005]. Furthermore, neuroimaging studies in humans support an involvement of the BNST rather in sustained anxiety [Alexander et al., 2010; Alvarez et al., 2011; Grupe et al., 2013; McMenamin et al., 2014; Somerville et al., 2010, 2013; Straube et al., 2007a] and of the amygdala in transient, phasic fear responses [Boehme et al., 2014b; Grupe et al., 2013; Lipka et al., 2011; Somerville et al., 2013]. In particular, several studies reported activation to the threat cue in the amygdala and during unpredictable anticipation of threat in the BNST within one and the same experiment [Alvarez et al., 2011; Grupe et al., 2013; Somerville et al., 2013]. However, these experiments could not differentiate whether the onset and offset of (briefly presented) threat-related cues or purely temporal factors (phasic onset versus sustained components) are responsible for the dissociation between activation in the amygdala and the BNST. A very recent fMRI study found different functional roles for both, the BNST and the amygdala [McMenamin et al., 2014], during anticipatory anxiety mainly depending on connectivity patterns. Nevertheless, there was no evidence of a phasic amygdala response in this study. Thus, a clear distinction between the time courses of amygdala and BNST activation to threat solely depending on a temporal factor (phasic versus sustained component) has not been shown so far.

Abbreviations

ACC	anterior cingulate cortex
BNST	bed nucleus of the stria terminalis
fMRI	functional magnetic resonance imaging
HRF	hemodynamic response function
OFC	orbitofrontal cortex
PFC	prefrontal cortex
PPI	psychophysiological interaction
ROIs	regions of interest

Beyond regional brain activation, connectivity analyses offer a deeper understanding of the functional interplay between different brain regions [Adhikari, 2014]. Concerning amygdala and BNST, patterns of activity and connectivity seem to be partly similar, as both regions are interconnected, receive similar neuronal input and project to the same target areas [see Fox et al., 2010; Walker et al., 2009]. Subregions of BNST and amygdala have been found to mediate both anxiolytic and anxiogenic effects [Tovote et al., 2015]. Moreover, different behavioral features of anxiety were shown to be modulated by distinct neural circuits [Kim et al., 2013]. While a growing number of studies indicate differential activation patterns of the amygdala and BNST, there is also preliminary evidence for different connectivity patterns of the amygdala and BNST [McMenamin et al., 2014]. There is strong evidence concerning an interplay between the amygdala and prefrontal brain areas in bottom-up and top-down processes, especially during threat processing [see Kim et al., 2011]. Accordingly, an increased functional coupling between activation of the amygdala and the prefrontal cortex has been shown, which is especially pronounced in highly anxious individuals [Vytal et al., 2014]. Furthermore, increased functional connectivity has been demonstrated between the amygdala and the visual cortex [e.g., Lipka et al., 2011; Ousdal et al., 2014], indicating that the perception and emotional processing of relevant stimuli might recruit the amygdala [LeDoux, 2000; Tamietto and de Gelder, 2010]. McMenamin and colleagues [2014] investigated differential network characteristics of BNST and amygdala in a threat versus safe condition. The amygdala showed increased connectivity with an executive control network (including dorsolateral prefrontal and parietal cortex areas) during a specific intermediate time window. BNST connectivity with the explored networks was not observed. However, using diffusion tensor imaging (DTI) and resting state fMRI in humans, structural and functional connectivity was found between BNST and basal ganglia structures, thalamus, hippocampus, periaqueductal gray, and medial prefrontal cortex [Avery et al., 2014; Torrisi et al., 2015]. In another study, greater coupling of activation was shown between BNST and insula as well as between BNST and medial prefrontal cortex in response to threat versus safe cues [Kinnison et al., 2012]. Medial prefrontal cortex was suggested to promote BNST activity and in turn the development of negative emotions [Motzkin et al., 2015]. Besides the mentioned brain areas, anxiety is consistently associated with hyperactivity of insula and anterior cingulate cortex [Chua et al., 1999; Kalisch et al., 2006; Straube et al., 2007a,b]. During fear and anxiety, ACC and insula are often found to be co-activated [Straube et al., 2007a,b], and are implicated in a network that is suggested to segregate salient information in order to initiate adaptive responses [Menon and Uddin, 2010].

The present study aimed to investigate temporal activation and connectivity patterns of the amygdala and BNST

during anticipatory threat. To investigate the issue of genuine temporally different activation profiles in amygdala and BNST, it is necessary to use a design in which (a) the possibility of occurrence of the threat stimulus is perceived to be high throughout the whole anticipation phase and (b) the same experimental context during the whole anticipation phase is given. Therefore, we used an anticipatory anxiety design with temporally unpredictable threat stimuli but constant presentation of the threat-signaling cue. Besides activation patterns of amygdala and BNST in response to the threat-signaling cue, we also investigated responses in areas that have previously been associated with anticipatory anxiety including anxiety-potentiated sensory processing [e.g. insula, prefrontal cortex (PFC) including orbitofrontal cortex (OFC), anterior cingulate cortex (ACC), thalamus, periaqueductal grey (PAG), and visual as well as auditory cortex areas; Dresler et al., 2013; Etkin and Wager, 2007; Grupe and Nitschke, 2013]. We hypothesized that the amygdala is more characterized by a brief phasic response to the threat cue, while the BNST and other areas show a more sustained response. This should also be evident in different connectivity patterns of the amygdala and BNST during phasic and sustained fear.

MATERIALS AND METHODS

Subjects

Forty-three healthy individuals recruited via public announcement participated in the study. Five participants had to be excluded from analyses because of head movements > 3 mm/° during functional scanning and technical problems during data acquisition in the scanner. Therefore, the final sample under study consisted of 38 participants (30 females, mean age $= 26.05 \pm 5.21$ years). All were right-handed with normal or corrected-to-normal vision and normal hearing, had no history of psychiatric disorders, and were free of psychotropic medication. The study was approved by the ethics committee of the University Hospital of Würzburg. After participants were given a complete description of the study and its procedures, written informed consent was obtained in accordance with the Declaration of Helsinki in its latest version from 2008.

Paradigm

Three aversive (human scream #275, 276, 277) and three neutral sounds (#370, 376, 377) from the International Affective Digital Sounds system [IADS; Bradley and Lang, 1999] were presented for 4 seconds during functional magnetic resonance imaging (fMRI). Loudness of the sounds was adjusted individually to maximal tolerable level. During fMRI, each sound was presented three times in a pseudo-random order with no more than two events of the same category following each other. Sounds were cued by either a square or circle that predicted the presentation of an aversive or a neutral sound (counter balanced across participants), respectively. The cue appeared 5 to 35 s (mean 23.33 s) prior to the sound and stayed on-screen during the whole anticipation phase. The intertrial interval lasted 15 s during which a white fixation cross on a black background was presented. During scanning, auditory stimuli were presented binaurally via headphones.

After scanning, participants rated all sounds and cues using a nine-point Likert scale [Self Assessment Manikin; Bradley and Lang, 1994] to assess valence (1 = very pleasant to 9 = very unpleasant, with 5 = neutral), arousal (1 = not arousing to 9 = very arousing), and threat (1 = not threatening to 9 = very threatening). Behavioral data were analyzed by repeated measures analysis of variance (ANOVA) and *t*-tests using the software SPSS (Version 22.0.0.0; SPSS, INC.). A probability level of $p < 0.05$ was considered statistically significant.

FMRI

BOLD (blood oxygen-level-dependent) responses and structural brain scans were recorded in a 3 Tesla magnetic resonance scanner ("Magnetom Skyra", Siemens, Medical Solutions, Erlangen, Germany). After a T1-weighted anatomical scan, a run of 386 volumes was acquired using a T2*-weighted echo-planar sequence (TE = 30 ms, flip angle = 90°, matrix = 64 × 64, FOV = 230 mm, TR = 2,000 ms). Each volume consisted of 35 axial slices (thickness = 3.5 mm, gap = 0 mm, in plane resolution = 3.6 × 3.6 mm, slice order = ascending). The first four volumes were discarded from analysis to ensure that steady-state tissue magnetization was reached.

FMRI data analysis was realized by using BrainVoyager QX (BVQX) software (Version 2.8; Brain Innovation, Maastricht, The Netherlands). At first, all volumes were realigned to the first volume. Then, a slice time correction was conducted. Further data preprocessing comprised spatial (5 mm full-width half-maximum isotropic Gaussian kernel) as well as temporal smoothing (high pass filter: 5 cycles per run; low pass filter: 2.8 s; linear trend removal). The anatomical and functional images were co-registered and normalized to the Talairach space [Talairach and Tournoux, 1988].

Statistical analyses were performed by multiple linear regression of the signal time course at each voxel. The expected BOLD signal change for each event type (predictor) was modeled by a hemodynamic response function (HRF). To investigate phasic and sustained activation patterns during the anticipation phases, two general linear models (GLM) were calculated. In the first GLM (phasic fear model), phasic responses were modeled as HRFs elicited by the first second of the aversive and neutral anticipation intervals, while the remaining anticipation time was modeled as a separate predictor (predictor of no interest). In the second GLM (sustained fear model), an HRF

TABLE 1. Ratings of valence, arousal, and anxiety of cues and sounds

	Valence		Arousal		Anxiety	
	Neutral	Aversive	Neutral	Aversive	Neutral	Aversive
Cues	3.66	4.87	2.58	3.68	1.84	3.55
	(1.21)	(1.99)	(1.48)	(2.32)	(1.33)	(2.27)
Sounds	3.76	7.96	2.89	7.62	2.05	6.25
	(1.13)	(0.91)	(1.25)	(1.12)	(1.19)	(2.03)

Mean and standard deviation (in parentheses) are displayed.

was modeled for the whole duration of aversive and neutral anticipation phases. In both GLMs, aversive and neutral cue phases were defined as events of interest and sounds as events of no interest. On the first level, predictor estimates based on z-standardized time course data were generated for each subject using a random-effects model with adjustment for autocorrelation following a global AR(1) model. On the second level, predictor estimates were analyzed across subjects according to planned contrasts. Analyses were conducted for specific regions of interest (ROIs). Following the approach recommended by Eickhoff et al. [2006], we extracted the amygdala ROI consisting of three bilateral amygdala maximum probability maps (laterobasal, centromedial, and superficial; 9,077 mm^3 in total) of the anatomy toolbox [Eickhoff et al., 2005]. ROIs for the bilateral insulae (32,822 mm^3), PFC (dorsolateral superior frontal gyrus: 68,467 mm^3, medial superior frontal gyrus: 44,945 mm^3, middle frontal gyrus: 86,708 mm^3), cingulate cortex (anterior: 23,963 mm^3, median: 36,632 mm^3), OFC (middle frontal gyrus, orbital part: 17,371 mm^3, inferior frontal gyrus, orbital part: 30,334 mm^3, superior frontal gyrus, orbital part: 14,199 mm^3), bilateral thalamus (18,926 mm^3), and auditory (superior temporal gyrus: 48,140 mm^3, Heschl gyrus: 4,484 mm^3) as well as sensory cortex areas (Cuneus: 26,335 mm^3, fusiform gyrus: 43,868) were extracted from the AAL atlas included in WFU PickAtlas software [Maldjian et al., 2004; Maldjian et al., 2003; Tzourio-Mazoyer et al., 2002]. Using MATLAB (Version 7.8; The MathWorks, Inc) all ROIs were transformed into BVQX-compatible Talairach coordinates via ICBM2tal [Lancaster et al., 2007]. ROIs for bilateral BNST (866 mm^3) and PAG (1,357 mm^3) were defined according to an anatomical atlas of the human brain [Mai et al., 1997].

Statistical parametric maps resulting from voxel-wise analyses were considered statistically significant for clusters that survived a correction for multiple comparisons. For this purpose, we used the approach as implemented in BVQX [see Goebel et al., 2006 based on a 3D extension of the randomization procedure described by Forman et al., 1995]. First, the voxel-level threshold was set at $p < 0.005$ (uncorrected). Thresholded maps were then submitted to a ROI-based correction criterion for multiple comparisons based on an estimate of map's spatial smoothness [Forman et al., 1995] and on an iterative procedure (Monte Carlo simulation). The Monte Carlo simulation used 1,000 iterations to estimate the minimum cluster-size threshold that yielded a cluster-level false-positive rate of 5%. The cluster-size thresholds were applied to the statistical maps.

Extraction of ROI time courses and convolution with model HRF for psychophysiological interaction (PPI) analyses were conducted with Neuroelf's (www.neuroelf.net) ComputeGLM method. Because of their relevance for aversive anticipation (see Results), we focused on significantly activated clusters from the ROI analyses in the right amygdala (105 mm^3) and right BNST (220 mm^3) as seed regions (ROI Results). Using the contrast aversive anticipation > neutral anticipation as psychological predictor and the respective signal time courses extracted from these two seed regions, we calculated PPI-GLMs in BVQX for the amygdala and BNST as seed regions, separately. Additionally, we calculated a phasic as well as a sustained PPI-GLM by defining a phasic (1s) as well as a sustained (whole duration) predictor containing different psychological functions with which the time course of the seeds was multiplied (see e.g. Friston et al., 1997). The sounds were defined as predictors of no interest.

RESULTS

Rating Data

Analyses of rating data showed that aversive versus neutral sound anticipation was rated as more negative ($t_{[37]} = 3.61$; $p < 0.001$), more arousing ($t_{[37]} = 3.41$; $p < 0.01$), and more anxiety-inducing ($t_{[37]} = 5.59$; $p < 0.001$). Similarly, aversive sounds in comparison to neutral sounds were rated as more negative ($t_{[37]} = 21.16$; $p < 0.001$), more arousing ($t_{[37]} = 20.16$; $p < 0.001$), and more anxiety-inducing ($t_{[37]} = 10.44$; $p < 0.001$). An overview of rating data is presented in Table 1.

fMRI Data

ROI results

Phasic fear. Modeling phasic responses at anticipation cue onset and comparing aversive > neutral anticipation

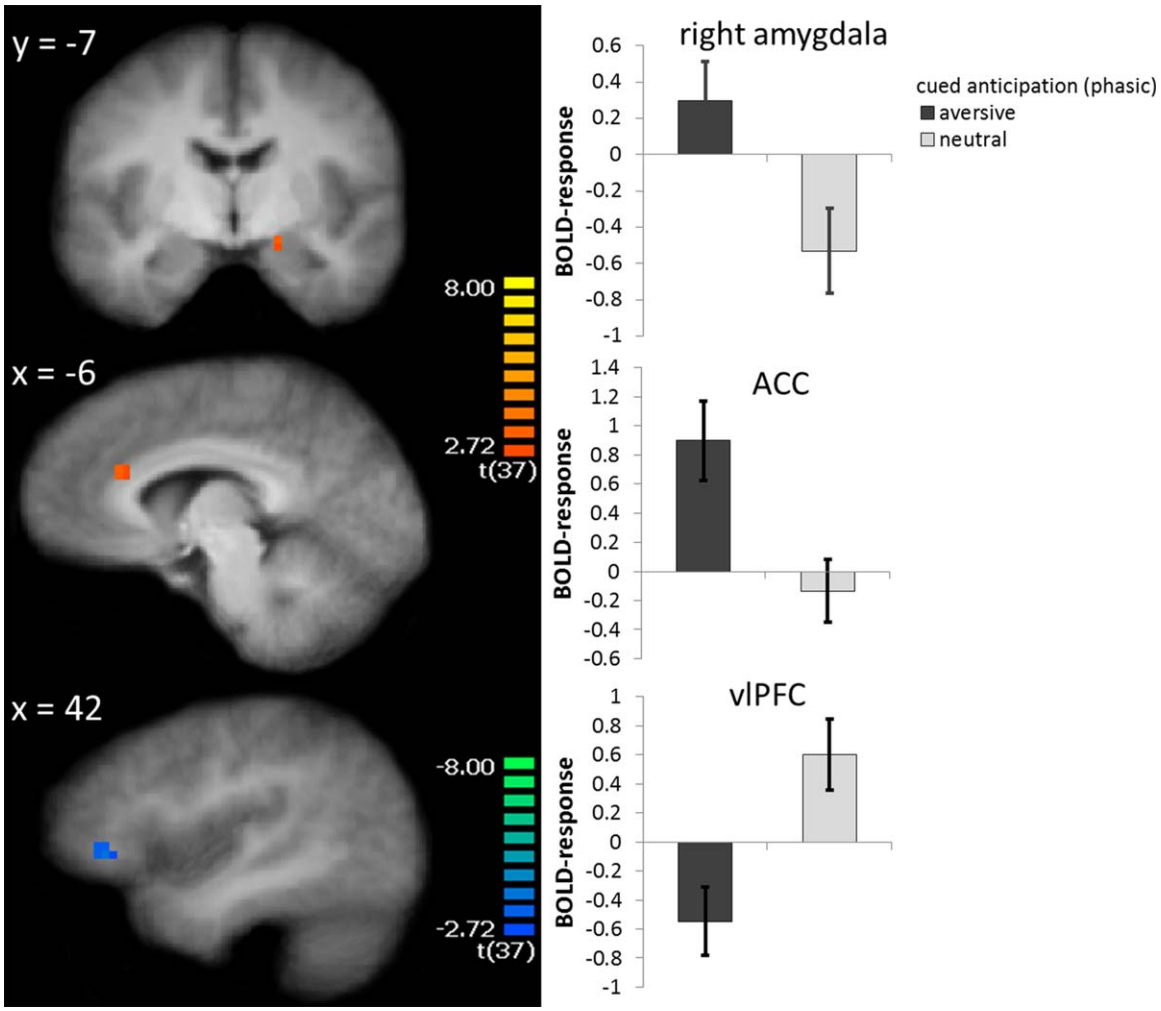

Figure 1.

Phasic fear: During the onset of anticipatory cues, participants showed increased activation to aversive vs. neutral cue onset in the right amygdala, anterior cingulate cortex (ACC), and decreased activation to aversive vs. neutral cue onset in the right ventrolateral prefrontal cortex (vlPFC). Statistical parametric maps are overlaid on an averaged T1 scan. The graphs on the right side display parameter estimates per condition (mean ± standard error for the maximally activated voxel). [Color figure can be viewed in the online issue, which is available at wileyonlinelibrary.com.]

revealed significant activation differences in the right amygdala (peak voxel Talairach coordinates: $x = 16$, $y = -7$, $z = -10$; voxel size 105 mm^3, $t_{[37]} = 3.49$), ACC (peak voxel Talairach coordinates: $x = -7$, $y = 27$, $z = 22$; voxel size 324 mm^3, $t_{[37]} = 3.44$), and ventrolateral prefrontal cortex (vlPFC; peak voxel Talairach coordinates: $x = 42$, $y = 34$, $z = 1$; voxel size 216 mm^3, $t_{[37]} = -4.03$; see Fig. 1).

Sustained fear. In the GLM that modeled the entire anticipation interval, several brain areas displayed an activation difference to aversive versus neutral sound anticipation. A greater activation to aversive in comparison to neutral anticipation was found in the right BNST (peak voxel Talairach coordinates: $x = 8$, $y = 0$, $z = 8$; voxel size 220 mm^3, $t_{[37]} = 4.85$), PAG (peak voxel Talairach coordinates: $x = 2$, $y = -26$, $z = -1$; voxel size 141 mm^3, $t_{[37]} = 4.49$), dorsolateral prefrontal cortex (dlPFC; left: peak voxel Talairach coordinates: $x = -27$, $y = 36$, $z = 35$; voxel size 2,970 mm^3, $t_{[37]} = 4.31$; right: peak voxel Talairach coordinates: $x = 39$, $y = 39$, $z = 21$; voxel size 6,642 mm^3, $t_{[37]} = 4.66$), insula (left: peak voxel Talairach coordinates: $x = -29$, $y = 14$, $z = -5$; voxel size 7,101 mm^3, $t_{[37]} = 5.48$; right: peak voxel Talairach coordinates: $x = 40$, $y = 20$, $z = 2$; voxel size 8,640 mm^3, $t_{[37]} = 5.61$), ACC (peak voxel Talairach coordinates: x = 6, y = 12, z = 38; voxel size 6,129 mm^3, $t = 5.63$), posterior cingulate cortex (PCC)/precuneus (left: peak voxel Talairach coordinates: $x = -11$,

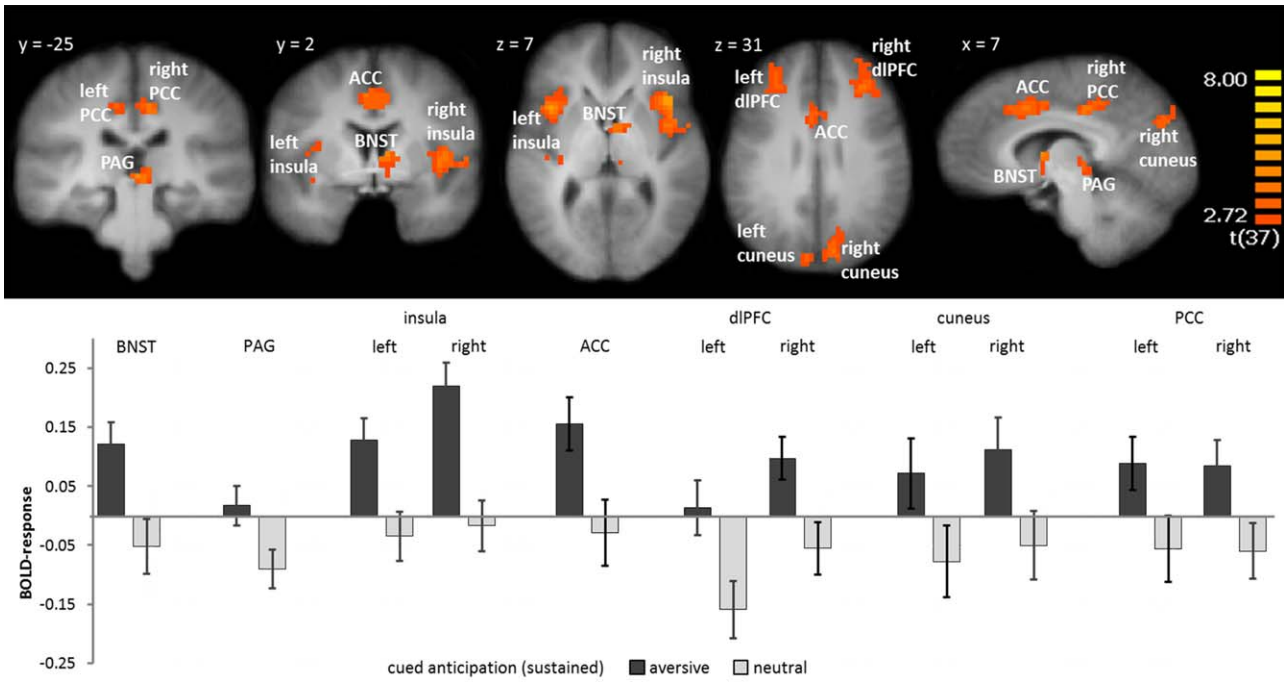

Figure 2.

Sustained fear: During the entire anticipation interval, participants showed greater activation in the right bed nucleus of stria terminalis (BNST), periaquaductal gray (PAG), left and right insula, anterior cingulate cortex (ACC), left and right dlPFC, cuneus, and posterior cingulate cortex (PCC) during the anticipation of aversive vs. neutral sounds. Statistical parametric maps are overlaid on an averaged T1 scan. The graph below displays parameter estimates per condition (mean ± standard error for the maximally activated voxel). [Color figure can be viewed in the online issue, which is available at wileyonlinelibrary.com.]

$y = -28$, $z = 38$; voxel size 324 mm^3, $t_{[37]} = 3.92$; right: peak voxel Talairach coordinates: $x = 9$, $y = -26$, $z = 37$; voxel size 1566 mm^3, $t_{[37]} = 4.39$), and cuneus (left: peak voxel Talairach coordinates: $x = -8$, $y = -84$, $z = 26$; voxel size 848 mm^3, $t_{[37]} = 3.84$; right: peak voxel Talairach coordinates: $x = 10$, $y = -78$, $z = 29$; voxel size 1,906 mm^3, $t_{[37]} = 4.07$). Results of the ROI-based analysis are displayed in Figure 2.

TABLE 2. Psychophysiological interaction of phasic and sustained response of the right amygdala

		Phasic response					Sustained response				
		Talairach					Talairach				
ROI	H	*x*	*y*	*z*	Size	*t*-value	*x*	*y*	*z*	Size	*t*-value
Frontal cortex											
dlPFC	L						−23	17	49	432	−3.69
Sensory cortex											
Auditory cortex (BA 42)	L	−62	−12	7	159	3.57					
Cuneus (BA 18)	L	−15	−63	17	692	4.43					
	R	16	−72	32	477	3.57	7	−62	17	197	−3.94
Fusiform gyrus (BA 37)	L	−35	−58	−13	1138	4.03	−36	−55	−14	1654	4.27
	R	34	−63	−20	224	4.02	25	−57	−14	410	3.60
Limbic regions											
Insula	R	33	2	10	108	3.39					

Abbreviations: ROI, region of interest; H, hemisphere; L, left; R, right; dlPFC, dorsolateral prefrontal cortex; BA, Brodmann area.

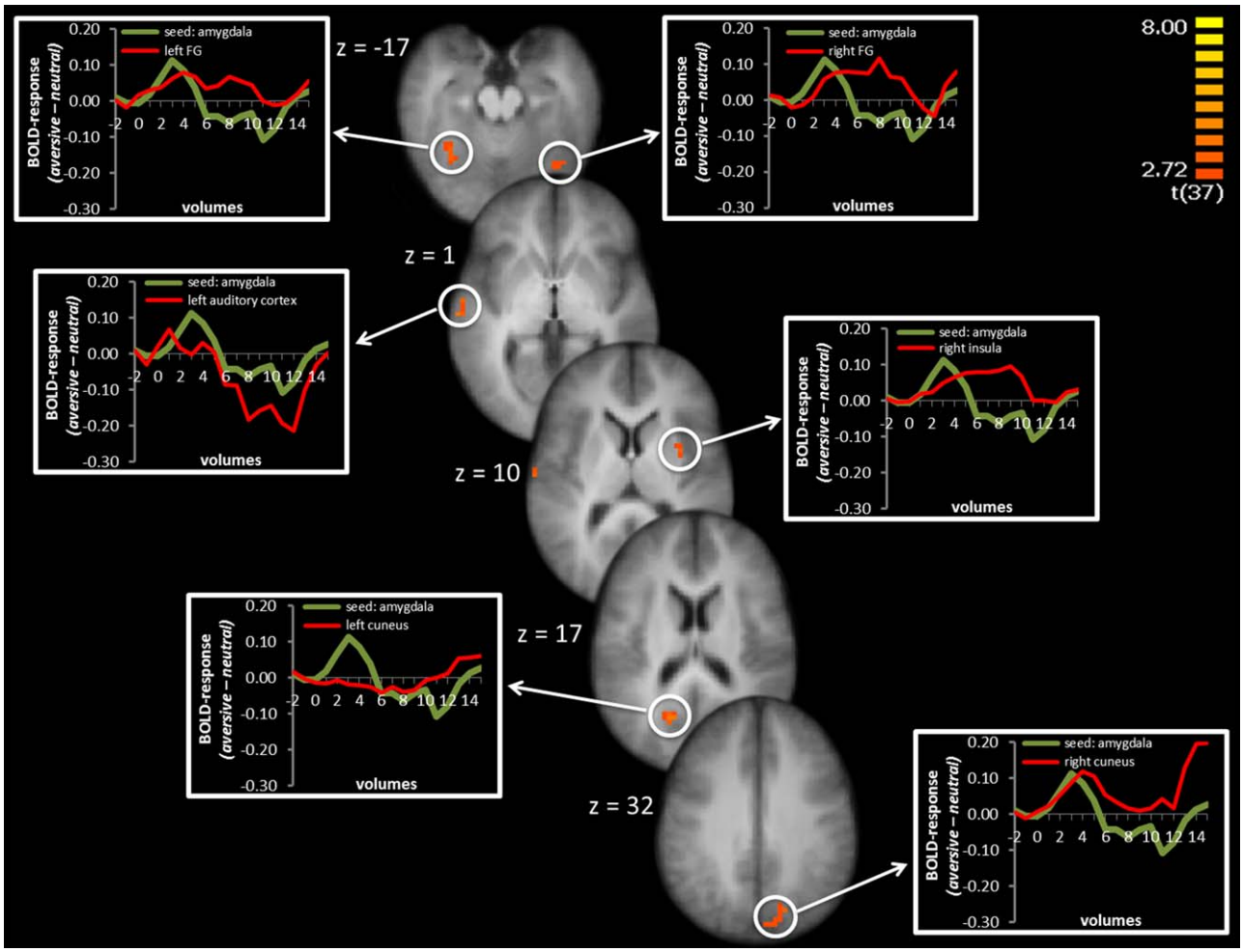

Figure 3.

Psychophysiological interaction of right amygdala seed: Phasic activation in the right amygdala was positively coupled with activation in left and right fusiform gyrus (FG), left auditory cortex, right insula, and left and right cuneus. Significant voxels are overlaid on an averaged T1 scan. Time courses of activation are shown in the graphs at the left and right side starting two volumes before cue presentation and the first 15 volumes of cue presentation. The green line displays the difference between aversive-neutral sound anticipation in the seed region and the red line display the difference between aversive-neutral sound anticipation in the co-activated brain region. [Color figure can be viewed in the online issue, which is available at wileyonlinelibrary.com.]

Functional connectivity

PPI with right amygdala seed. The amygdala seed comprised all voxels of the amygdala cluster resulting from analysis of the phasic fear model as reported above. The phasic time course of activation in these voxels was positively associated with the activation in several sensory cortex areas (auditory cortex, cuneus, and the fusiform gyrus). Additionally, we found a positive association with activation of the right insula (Table 2 and Fig. 3). For the sake of completeness, we also tested PPI of the activation during the whole anticipation period for the amygdala seed. This revealed a positive co-activation pattern of the amygdala and the bilateral fusiform gyrus as well as the dlPFC. However, sustained activation in the right cuneus was negatively coupled with sustained amygdala activation (Table 2).

PPI with right BNST seed. Sustained activation of voxels that showed significantly greater activation to anticipation of aversive versus neutral sounds in the right BNST showed negative psychophysiological interaction with the activation in left and right cuneus, and a positive association with bilateral insula and left thalamus (Table 3 and Fig. 4). We also examined PPI of phasic BNST activation. This revealed a positive co-activation in frontal areas (including ACC, dlPFC, and vlPFC), amygdala, and insula. Activation in visual cortex areas was negatively co-activated with BNST activation (Table 3).

TABLE 3. Psychophysiological interaction of phasic and sustained response of the right BNST

		Phasic response					Sustained response				
		Talairach					Talairach				
ROI	H	*X*	*y*	*z*	Size	*t*-value	*x*	*y*	*z*	Size	*t*-value
Frontal cortex											
dlPFC	R	27	13	46	1134	3.71					
	R	45	3	47	135	3.20					
vlPFC	R	36	40	6	324	3.57					
ACC	M	10	26	31	189	3.65					
Sensory cortex											
Cuneus (BA 18)	L	−15	−85	20	459	−4.40	−5	−78	17	216	−2.95
	R	14	−90	26	270	−4.35	13	−63	16	139	−3.53
Fusiform gyrus (BA 37)	R	18	−76	−15	190	−3.22					
Limbic regions											
Amygdala	R	15	−7	−15	81	3.43					
Insula	L	−32	5	12	108	3.24	−29	24	4	189	4.43
	R	36	12	−2	162	3.53	31	18	7	162	3.25
Thalamus	L						−17	−21	0	162	3.34

Abbreviations: ROI, region of interest; H, hemisphere; L, left; R: right; M, medial; dlPFC, dorsolateral prefrontal cortex; vlPFC, ventrolateral prefrontal cortex; BA: Brodmann area.

DISCUSSION

The aim of the present study was to investigate temporal activation profiles of the amygdala and the BNST as well as further brain regions during cue-induced anticipatory anxiety. Furthermore, we explored connectivity patterns of the amygdala and BNST during anticipatory threat. As hypothesized, modeling phasic responses at cue onset revealed significant hyperactivation in the amygdala. Modeling the entire anticipation interval revealed significant activation in the BNST. Analyses of functional connectivity showed separate connectivity patterns for amygdala and BNST that differ for phasic and sustained fear. Thus, the present study supports the assumption that amygdala and BNST are differentially involved in phasic and sustained responses during threat anticipation based on differential activation and connectivity profiles.

Our results indicate a phasic amygdala response even though the cue is present during the whole anticipation interval. Related to this, a habituation of amygdala hyperactivation was shown during repeated [e.g., Straube et al., 2007b; Wendt et al., 2012] and even within-trial threat exposure [Phelps et al., 2001]. This is in accordance with the assumed role of the amygdala in the processing of highly salient stimuli, especially in the rapid detection of threat and initiation of active defensive behaviors [LeDoux, 1998; Öhman and Mineka, 2001].

Interestingly, a recent study by Plichta et al. [2014] showed that the session-wise amygdala habituation had a higher retest reliability than the evoked amygdala amplitude. Although our design was not suitable to detect habituation over the session, further studies should consider amygdala habituation as an additional measurement of interindividual differences in context of phasic and sustained fear.

Furthermore, there is evidence that amygdala activation is associated with activation in sensory cortices and that the amygdala possibly modulates perceptual processing via back projections to these areas [Amaral et al., 2003; Freese and Amaral, 2005; Vuilleumier et al., 2002]. Accordingly, our analysis of functional connectivity showed a positive association between the activation in the amygdala and several sensory brain areas (including auditory and visual cortex), especially during phasic response. Hence, our results support a central role of the amygdala in an alerting response system and the modulation of perceptual and emotional processing of relevant stimuli [LeDoux, 2000; Lipka et al., 2011; Pessoa and Adolphs, 2010; Tamietto and de Gelder, 2010], possibly by preferential processing of salient information [Grupe and Nitschke, 2013] especially in a phasic manner [see also Mueller et al., 2009].

Although there is a great body of animal studies that indicate a critical role of the BNST in sustained fear [e.g., Fendt et al., 2003; Hammack et al., 2004; Kalin et al., 2005; Waddell et al., 2006], the characteristic function of the BNST in the mediation of sustained fear in humans as well as the exact temporal activation profiles in relation to the amygdala were not clear. Since the BNST has been shown to be involved in anticipatory anxiety in humans [Straube et al., 2007a], several studies supported this finding of BNST activation in humans during sustained fear [Alexander et al., 2010; Alvarez et al., 2011; Grupe et al., 2013; McMenamin et al., 2014; Somerville et al., 2013], even though using different approaches with different possible conclusions. For example, the study by Grupe and colleagues [2013] investigated the temporal characteristics of brain activation to phasic versus sustained brain responses during anticipation of aversive and neutral

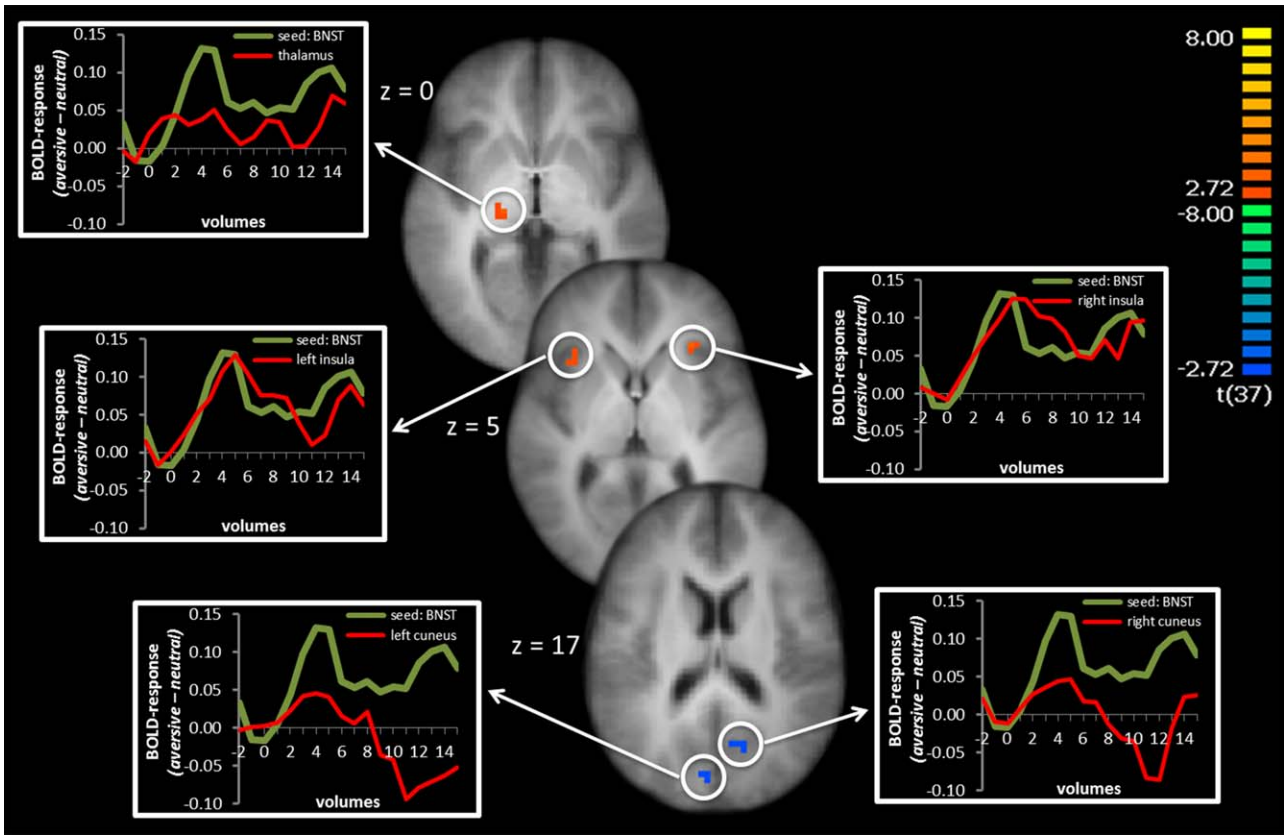

Figure 4.

Psychophysiological interaction of right BNST seed: Sustained activation in the right BNST was positively coupled with activation in the left thalamus and left and right insula and negatively associated with activation in the left and right cuneus. Significant voxels are overlaid on an averaged T1 scan. Time courses of activation are shown in the graphs at the left and right side starting two volumes before cue onset. The green line displays the difference between aversive-neutral sound anticipation in the seed region and the red line displays the difference between aversive-neutral sound anticipation in the co-activated brain region. [Color figure can be viewed in the online issue, which is available at wileyonlinelibrary.com.]

pictures. However, in this study a brief threat cue was shown followed by a fixation cross during a brief anticipation interval. The authors observed cue-associated responses in regions associated with threat detection and early processing of predictive cues, including the amygdala, OFC, and pregenual ACC, but only for individuals with elevated anxiety symptoms. The authors argued that a stronger phasic amygdala effect might be seen across all individuals with the use of a more aversive stimulus that induces greater anticipatory anxiety. In this study, sustained anticipatory responses during the fixation cross were observed in the BNST, insula, and PAG. McMenamin and colleagues [2014] investigated phasic, intermediate, and sustained activation patterns in an electric shock versus no shock anticipation paradigm. They observed no phasic amygdala response. Furthermore and similar to our results, activation differences in BNST, insula, prefrontal cortex, and PCC were more pronounced in later phases of threat anticipation. Alvarez and colleagues [2011] reported phasic amygdala activation to cues that predict shock and additionally sustained BNST activation during unpredictable shock anticipation. However, in this study, the BNST also showed a phasic response to the onset of the unpredictable block. Somerville et al. [2013] showed a transient response in the amygdala and PAG to negative pictures and a sustained response in BNST and insula. All these studies differ in characteristics concerning the anticipation period (predictability in duration and assurance of occurrence, presentation of threatening stimuli within [NPU paradigms] versus after anticipation block) and anticipated threatening stimuli (pictures, electric shocks), but most studies failed to differentiate phasic (onset) and sustained (whole duration) response to one and the same anticipation cue. Increasing evidence exists to segregate anxiety response in phasic and sustained response patterns which our study strongly supports.

Furthermore, our results indicate a differential functional connectivity pattern for the amygdala and BNST. Whereas the amygdala was functionally interconnected primarily with sensory brain regions, especially in response to the onset of the threat cue (see above), the onset BNST activation was functionally connected with frontal areas. A functional connectivity of amygdala and PFC activation was restricted to sustained activation patterns. In contrast to McMenamin et al. [2014] who found an increased association of intermediate activity in the amygdala and the executive control network (including dorsolateral prefrontal and parietal cortex areas), we found negatively coupled co-activation of the amygdala and dlPFC. This possibly reflects a sustained top-down-regulation of amygdala hyperactivation [e.g., Kim et al., 2011].

There was also a significant functional connectivity between the sustained BNST response and thalamus. This is in accordance with the results of Avery and colleagues [2014], who showed structural connectivity between BNST and thalamus. However, functional connectivity of these regions has not been reported in previous studies [Kinnison et al., 2012; McMenamin et al., 2014]. Our results, however, underscore the assumption that the BNST-thalamus pathway constitutes a relevant circuit essential for sustained fear processes since the thalamus seems to be essentially involved in arousal and states of vigilance [e.g., Llinás and Steriade, 2006] and also in visual salience or attention [Grieve et al., 2000]. This indicates that the BNST also may modulate (possibly via the thalamus) the processing of salient stimuli, especially in the sensory cortex, but in a different manner compared to the amygdala's proposed influence.

Finally, insula activation was positively associated with activation in amygdala and BNST and the interplay with the right insula activation seems to be the only overlap of the two examined connectivity networks. The insula has been implicated in interoception [Craig, 2002] and as involved in anticipatory anxiety [e.g., Boehme et al., 2014b; Paulus and Stein, 2006; Simmons et al., 2006; Straube et al., 2007a]. Although previous studies [e.g., Boehme et al., 2014b; Paulus and Stein, 2006] and the current results suggest a sustained response in this region, the insular hyperactivation seems to develop during the stimulus onset and to co-vary with amygdala responses. This is in accordance with a study done by Carlson et al. [2011] who reported coactivated amygdala and insula in high trait anxious participants, especially when the anticipated event was close.

Besides activation in amygdala and BNST, we also found activations in other brain regions. Interestingly, we found a phasic deactivation in right vlPFC for aversive compared with neutral condition and therefore higher activation for neutral compared to aversive condition (see Fig. 1). Similarly, McMenamin et al. [2014] reported a phasic prefrontal deactivation. The activation in vlPFC may reflect effort to downregulate emotions, as indicated by the study by Klumpers et al. [2015]. In this study the authors described higher brain vlPFC activation to threat offset via an implicit emotion regulation instruction. Furthermore, a sustained response was found in regions that have previously been shown to be involved in interoception [insula; Craig, 2002], the regulation of anxiety and autonomic functions [PAG; Linnman et al., 2012], selective attention and executive functions [ACC, dlPFC; Forster et al., 2015; Pessoa, 2008], and primary vision (cuneus). Furthermore, different clusters of the ACC were significantly activated during phasic and during sustained modeling, indicating an early onset of ACC hyperactivation that increase in cluster and effect size during sustained fear [see also Boehme et al., 2014]. The activation pattern of these regions are in accordance with previous studies examining phasic and sustained fear responses in the brain [e.g., Alvarez et al., 2011; Grupe et al., 2013; McMenamin et al., 2014; Somerville et al., 2013].

At the end, we would like to mention some limitations of our study. We did not assess a behavioral measure which comes along with difficulties to segregate phasic and sustained fear. Additionally, we did not focus on different genotypes that were evidenced to be associated with fear and anxiety and possibly comes along with different abnormalities in threat processing that might be vulnerable to the development of clinical anxiety. Furthermore, the used paradigm did not permit quantification of predictable and unpredictable occurrence of threat, which is often associated with phasic and sustained fear concepts. Upcoming studies should account for this and integrate behavioral measures, skin conductance for example, as well as the investigation of different genotypes and the manipulation of timely predictability of upcoming threat. Furthermore, analyses were performed to detect whether time course of brain activation is phasic or sustained by conducting a GLM with either an onset or an entire predictor. We focused on these two predictors because of existing literature so far. But also other types of activation pattern are possible, e.g. the time course of activation in the BNST seems to show both a phasic as well as sustained component. Nevertheless, the phasic activation did not reach significance. Future studies need to take differential patterns of brain activation in account.

CONCLUSIONS

To sum up, the results of our study indicate amygdala activation to be more phasic and BNST activation to be more sustained during cued anticipation of threat. Activation patterns of further brain regions previously associated with anxious processing are in accordance with similar studies on anticipatory anxiety. Moreover, connectivity analyses suggest that amygdala and BNST operate within distinct networks during anticipatory anxiety.

REFERENCES

Adhikari A (2014): Distributed circuits underlying anxiety. Front Behav Neurosci 8:112

Alexander N, Osinsky R, Schmitz A, Mueller E, Kuepper Y, Hennig J (2010): The BDNF Val66Met polymorphism affects HPA-axis reactivity to acute stress. Psychoneuroendocrinology 35:949–953.

Alvarez RP, Chen G, Bodurka J, Kaplan R, Grillon C (2011): Phasic and sustained fear in humans elicits distinct patterns of brain activity. NeuroImage 55:389–400.

Amaral DG, Behniea H, Kelly JL (2003): Topographic organization of projections from the amygdala to the visual cortex in the macaque monkey. Neuroscience 118:1099–1120.

Avery SN, Clauss JA, Winder DG, Woodward N, Heckers S, Blackford JU (2014): BNST neurocircuitry in humans. NeuroImage 91:311–323.

Boehme S, Mohr A, Becker M, Miltner W, Straube T (2014a): Area-dependent time courses of brain activation during video-induced symptom provocation in social anxiety disorder. Biol Mood Anxiety Disord 4:6

Boehme S, Ritter V, Tefikow S, Stangier U, Strauss B, Miltner WH, Straube T (2014b): Brain activation during anticipatory anxiety in social anxiety disorder. Soc Cogn Affect Neurosci 9:1413–1418.

Bradley M, Lang PJ (1999): The International affective digitized sounds (IADS): stimuli, instruction manual and affective ratings: NIMH Center for the Study of Emotion and Attention.

Bradley MM, Lang PJ (1994): Measuring emotion: The self-assessment manikin and the semantic differential. J Behav Ther Exp Psychiatry 25:49–59.

Carlson JM, Greenberg T, Rubin D, Mujica-Parodi LR (2011): Feeling anxious: anticipatory amygdalo-insular response predicts the feeling of anxious anticipation. Soc Cogn Affect Neurosci 6:74–81.

Casada JH, Dafny N (1991): Restraint and stimulation of bed nucleus of the stria terminalis produce similar stress-like behaviors. Brain Res Bull 27:207–212.

Craig AD (2002): How do you feel? Interoception: The sense of the physiological condition of the body. Nat Rev Neurosci 3: 655–666.

Davis M, Walker DL, Miles L, Grillon C (2009): Phasic vs sustained fear in rats and humans: Role of the extended amygdala in fear vs anxiety. Neuropsychopharmacology 35:105–135.

Dresler T, Guhn A, Tupak SV, Ehlis AC, Herrmann MJ, Fallgatter AJ, Deckert J, Domschke K (2013): Revise the revised? New dimensions of the neuroanatomical hypothesis of panic disorder. J Neural Transm 120:3–29.

Dunn JD (1987): Plasma corticosterone responses to electrical stimulation of the bed nucleus of the stria terminalis. Brain Res 407:327–331.

Duvarci S, Bauer EP, Paré D (2009): The bed nucleus of the stria terminalis mediates inter-individual variations in anxiety and fear. J Neurosci 29:10357–10361.

Eickhoff SB, Heim S, Zilles K, Amunts K (2006): Testing anatomically specified hypotheses in functional imaging using cytoarchitectonic maps. NeuroImage 32:570–582.

Eickhoff SB, Stephan KE, Mohlberg H, Grefkes C, Fink GR, Amunts K, Zilles K (2005): A new SPM toolbox for combining probabilistic cytoarchitectonic maps and functional imaging data. NeuroImage 25:1325–1335.

Etkin A, Wager TD (2007): Functional neuroimaging of anxiety: A meta-analysis of emotional processing in PTSD, social anxiety disorder, and specific phobia. Am J Psychiatry 164:1476–1488.

Fendt M, Endres T, Apfelbach R (2003): Temporary inactivation of the bed nucleus of the stria terminalis but not of the amygdala blocks freezing induced by trimethylthiazoline, a component of Fox Feces. J Neurosci 23:23–28.

Forman SD, Cohen JD, Fitzgerald M, Eddy WF, Mintun MA, Noll DC (1995): Improved assessment of significant activation in functional magnetic resonance imaging (fMRI): Use of a cluster-size threshold. Magn Reson Med 33:636–647.

Forster S, Nunez Elizalde AO, Castle E, Bishop SJ (2015): Unraveling the anxious mind: Anxiety, worry, and frontal engagement in sustained attention versus off-task processing. Cereb Cortex 25:609–618.

Fox AS, Shelton SE, Oakes TR, Converse AK, Davidson RJ, Kalin NH (2010): Orbitofrontal cortex lesions alter anxiety-related activity in the primate bed nucleus of stria terminalis. J Neurosci 30:7023–7027.

Freese JL, Amaral DG (2005): The organization of projections from the amygdala to visual cortical areas TE and V1 in the macaque monkey. J Comp Neurol 486:295–317.

Friston KJ, Buechel C, Fink GR, Morris J, Rolls E, Dolan RJ (1997): Psychophysiological and modulatory interactions in neuroimaging. NeuroImage 6:218–229.

Goebel R, Esposito F, Formisano E (2006): Analysis of functional image analysis contest (FIAC) data with brainvoyager QX: From single-subject to cortically aligned group general linear model analysis and self-organizing group independent component analysis. Hum Brain Mapp 27:392–401.

Grieve KL, Acuña C, Cudeiro J (2000): The primate pulvinar nuclei: Vision and action. Trends Neurosci 23:35–39.

Grupe DW, Nitschke JB (2013): Uncertainty and anticipation in anxiety: an integrated neurobiological and psychological perspective. Nat Rev Neurosci 14:488–501.

Grupe DW, Oathes DJ, Nitschke JB (2013): Dissecting the anticipation of aversion reveals dissociable neural networks. Cereb Cortex 23:1874–1883.

Hammack SE, Richey KJ, Watkins LR, Maier SF (2004): Chemical lesion of the bed nucleus of the stria terminalis blocks the behavioral consequences of uncontrollable stress. Behav Neurosci 118:443–448.

Kalisch R, Wiech K, Critchley HD, Dolan RJ (2006): Levels of appraisal: A medial prefrontal role in high-level appraisal of emotional material. Neuroimage 30:1458–1466.

Kalin NH, Shelton SE, Fox AS, Oakes TR, Davidson RJ (2005): Brain regions associated with the expression and contextual regulation of anxiety in primates. Biol Psychiatry 58:796–804.

Kim MJ, Loucks RA, Palmer AL, Brown AC, Solomon KM, Marchante AN, Whalen PJ (2011): The structural and functional connectivity of the amygdala: From normal emotion to pathological anxiety. Behav Brain Res 2:403–410.

Kim SY, Adhikari A, Lee SY, Marshel JH, Kim CK, Mallory CS, Lo M, Pak S, Mattis J, Lim BK, Malenka RC, Warden MR, Neve R, Tye KM, Deisseroth K (2013): Diverging neural pathways assemble a behavioural state from separable features in anxiety Nature 496:219–223.

Kinnison J, Padmala S, Choi J-M, Pessoa L (2012): Network analysis reveals increased integration during emotional and motivational processing. J Neurosci 32:8361–8372.

Klumpers F, Kroes MC, Heitland I, Everaerd D, Akkermans SE, Oosting RS, van Wingen G, Franke B, Kenemans JL, Fernandez G, Bass JM. (2015): Dorsomedial prefrontal cortex mediates the impact of serotonin transporter linked polymorphic region genotype on anticipatory threat reactions. Biol Psychiatry 78:582–589.

Lancaster JL, Tordesillas-Gutiérrez D, Martinez M, Salinas F, Evans A, Zilles K, Mazziotta JC, Fox PT (2007): Bias between MNI and Talairach coordinates analyzed using the ICBM-152 brain template. Hum Brain Mapp 28:1194–1205.

LeDoux J (1998): Fear and the brain: Where have we been, and where are we going? Biol Psychiatry 44:1229 –1238.

LeDoux J (2000): Emotion circuits in the brain. Annu Rev Neurosci 23:155–184.

Linnman C, Moulton EA, Barmettler G, Becerra L, Borsook D (2012): Neuroimaging of the periaqueductal gray: State of the field. NeuroImage 60:505–522.

Lipka J, Miltner W Straube T (2011): Vigilance for threat interacts with amygdala responses to subliminal threat cues in specific phobia. Biol Psychiatry 70:472–478.

Llinás RR, Steriade M (2006): Bursting of Thalamic Neurons and States of Vigilance. pp 3297–3308.

Lungwitz EA, Molosh A, Johnson PL, Harvey BP, Dirks RC, Dietrich A, Minick P, Shekhar A, Truitt WA (2012): Orexin-A induces anxiety-like behavior through interactions with glutamatergic receptors in the bed nucleus of the stria terminalis of rats. Physiol Behav 107:726–732.

Mai J, Assheuer J, Paxinos G. 1997. Atlas of the Human Brain. San Diago: Academic Press.

Maldjian JA, Laurienti PJ, Burdette JH (2004): Precentral gyrus discrepancy in electronic versions of the Talairach atlas. NeuroImage 21:450–455.

Maldjian JA, Laurienti PJ, Kraft RA, Burdette JH (2003): An automated method for neuroanatomic and cytoarchitectonic atlas-based interrogation of fMRI data sets. NeuroImage 19:1233–1239.

McMenamin BW, Langeslag SJE, Sirbu M, Padmala S, Pessoa L (2014): Network organization unfolds over time during periods of anxious anticipation. J Neurosci 34:11261–11273.

Menon V, Uddin LQ (2010): Saliency switching attention and control: a network model of insula function. Brain Struct Funct 214:655–667.

Mueller EM, Hofmann SG, Santesso DL, Meuret AE, Bitran S, Pizzagalli DA (2009): Electrophysiological evidence of attentional biases in social anxiety disorder. Psychol Med 39:1141–1152.

Öhman A, Mineka S (2001): Fears, phobias, and preparedness: toward an evolved module of fear and fear learning. Psychological Review 108:483–522.

Ousdal OT, Andreassen OA, Server A, Jensen J (2014): Increased amygdala and visual cortex activity and functional connectivity towards stimulus novelty is associated with state anxiety. PLoS One 9:e96146

Paulus MP, Stein MB (2006): An insular view of anxiety. Biol Psychiatry 60:383–387.

Pessoa L (2008): On the relationship between emotion and cognition. Nat Rev Neurosci 9:148–158.

Pessoa L, Adolphs R (2010): Emotion processing and the amygdala: from a 'low road' to 'many roads' of evaluating biological significance. Nat Rev Neurosci 11:773–783.

Phelps EA, O'Connor KJ, Gatenby JC, Gore JC, Grillon C, Davis M (2001): Activation of the left amygdala to a cognitive representation of fear. Nat Neurosci 4:437–441.

Plichta MM, Grimm O, Morgen K, Mier D, Sauer C, Haddad L, Tost H, Esslinger C, Kirsch P, Schwarz AJ, Meyer-Lindenberg A (2014): Amygdala habituation: A reliable fMRI phenotype. NeuroImage 103:383–390.

Simmons A, Strigo I, Matthews SC, Paulus MP, Stein MB (2006): Anticipation of aversive visual stimuli is associated with increased insula activation in anxiety-prone subjects. Biol Psychiatry 60:402–409.

Sink KS, Davis M, Walker DL (2013): CGRP antagonist infused into the bed nucleus of the stria terminalis impairs the acquisition and expression of context but not discretely cued fear. Learn Memory 20:730–739.

Sink KS, Walker DL, Yang Y, Davis M (2011): Calcitonin gene-related peptide in the bed nucleus of the stria terminalis produces an anxiety-like pattern of behavior and increases neural activation in anxiety-related structures. J Neurosci 31:1802–1810.

Somerville LH, Wagner DD, Wig GS, Moran JM, Whalen PJ, Kelley WM (2013): Interactions between transient and sustained neural signals support the generation and regulation of anxious emotion. Cereb Cortex 23:49–60.

Somerville LH, Whalen PJ, Kelley WM (2010): Human bed nucleus of the stria terminalis indexes hypervigilant threat monitoring. Biol Psychiatry 68:416–424.

Straube T, Mentzel H, Miltner W (2007a): Waiting for spiders: Brain activation during anticipatory anxiety in spider phobics. Neuroimage 37:1427–1436.

Straube T, Weiss T, Mentzel H, Miltner W (2007b): Time course of amygdala activation during aversive conditioning depends on attention. Neuroimage 34:462 –469.

Talairach J, Tournoux P. 1988. Co-Planar Stereotaxic Atlas of the Human Brain. 3-Dimensional Proportional System: An Approach to Cerebral Imaging. Stutgart: Thieme.

Tamietto M, de Gelder B (2010): Neural bases of the non-conscious perception of emotional signals. Nat Rev Neurosci 11:697–709.

Tzourio-Mazoyer N, Landeau B, Papathanassiou D, Crivello F, Etard O, Delcroix N, Mazoyer B, Joliot M (2002): Automated anatomical labeling of activations in spm using a macroscopic anatomical parcellation of the MNI MRI single-subject brain. NeuroImage 15:273–289.

Vuilleumier P, Armony JL, Clarke K, Husain M, Driver J, Dolan RJ (2002): Neural response to emotional faces with and without awareness: event-related fMRI in a parietal patient with visual extinction and spatial neglect. Neuropsychologia 40: 2156–2166.

Vytal KE, Overstreet C, Charney DR, Robinson OJ, Grillon C (2014): Sustained anxiety increases amygdala-dorsomedial prefrontal coupling: A mechanism for maintaining an anxious state in healthy adults. J Psychiatry Neurosci 39:321–329.

Waddell J, Morris RW, Bouton ME (2006): Effects of bed nucleus of the stria terminalis lesions on conditioned anxiety: Aversive conditioning with long-duration conditional stimuli and reinstatement of extinguished fear. Behav Neurosci 120:324–336.

Walker DL, Miles LA, Davis M (2009): Selective participation of the bed nucleus of the stria terminalis and CRF in sustained anxiety-like versus phasic fear-like responses. Prog Neuro-Psychopharmacol Biol Psychiatry 33:1291–1308.

Walker DL, Toufexis DJ, Davis M (2003): Role of the bed nucleus of the stria terminalis versus the amygdala in fear, stress, and anxiety. Eur J Pharmacol 463:199–216.

Wendt J, Schmidt LE, Lotze M, Hamm AO (2012): Mechanisms of change: Effects of repetitive exposure to feared stimuli on the brain's fear network. Psychophysiology 49:1319–1329.